Child's Nervous System (2019) 35:1251–1255
https://doi.org/10.1007/s00381-019-04113-3

CASE REPORT

Posterior fossa astroblastoma in a child: a case report and a review of the literature

Özlem Yapıcıer[1] · Mustafa Kemal Demir[2] · Umut Özdamarlar[2] · Deniz Kılıç[3] · Akın Akakın[4] · Türker Kılıç[4]

Received: 2 January 2019 / Accepted: 5 March 2019 / Published online: 12 March 2019

Abstract

A 4-year-old girl presented to the hospital with a progressive headache, difficulty walking, and persistent daily vomiting for 3 weeks. Papilledema was observed on fundoscopic examination. A large left cerebellovermian tumor with "bubbly" appearance was discovered. Total removal of the tumor mass was performed, and a diagnosis of low-grade astroblastoma was made. Adjuvant radiotherapy was performed due to the risk of recurrence. The patient is disease-free and has been kept on close follow-up for 6 months. The occurrence of posterior fossa astroblastoma has been rarely reported in the literature. Thus, when a "bubby" appearance enhancing cystic solid tumor is located on the cerebellar hemisphere in a child, an astroblastoma should also be included in the differential diagnosis.

Keywords Astroblastoma · Pediatric · Cerebellum · Diagnosis

Introduction

Astroblastomas (ABs) are uncommon neuroepithelial central nervous system (CNS) tumors that are usually found in the cortex of the cerebral hemispheres. They usually show a bimodal age distribution with a peak prevalence in children aged 5 to 10 and in young adults between 21 and 30 years [1, 2]. Astroblastoma accounts for 0.45–2.8% of gliomas [3]. It was described first by Bailey and Cushing in 1926 and further characterized by Bailey and Bucy in 1930 [4, 5].

The rare occurrence and the resemblance of imaging and histopathologic features of the disease to other glial tumors generally pose a diagnostic challenge. Here, we present an extremely rare case of a cerebellar AB in a 4-year-old female. The clinical presentation, magnetic resonance imaging (MRI), pathological, and therapeutic features this rare neoplasm are discussed with a review of posterior fossa involvement.

Case report

A 4-year-old female was admitted to our hospital with progressive headache, difficulty walking, and persistent daily vomiting for 3 weeks. Papilledema was observed on fundoscopic examination. Her Karnofsky performance scale (KPS) score was 90. The brain MRI demonstrated a large (52 × 48 × 51 mm), well-marginated left cerebellovermian "bubbly" mass with a mild perifocal edema, compressing the fourth ventricle. There were marked intratumoral hypointense signals on T1-weighted, T2-weighted, and susceptibility-weighted images (SWIs) secondary to dense globular calcifications. The tumor was predominantly iso- and hyperintense on T2-weighted images, and iso- and hypointense on T1-weighted images. The solid portions and the walls of internal cystic components of the tumor showed intense enhancement on postcontrast T1-weighted images. The tumor had a nonenhancing attached cystic component. There was no

✉ Mustafa Kemal Demir
demir.m.k@gmail.com

[1] Department of Pathology, Bahçeşehir University School of Medicine, Göztepe Medical Park Training and Education Hospital, Istanbul, Turkey

[2] Department of Radiology,, Bahçeşehir University School of Medicine, Göztepe Medical Park Training and Education Hospital, 11. kisim, Yasemin Apt, D blok. Daire 35 Ataköy, 34158 Istanbul, Turkey

[3] Bahçeşehir University School of Medicine, Istanbul, Turkey

[4] Department of Neurosurgery, Bahçeşehir University School of Medicine, Göztepe Medical Park Training and Education Hospital, Istanbul, Turkey

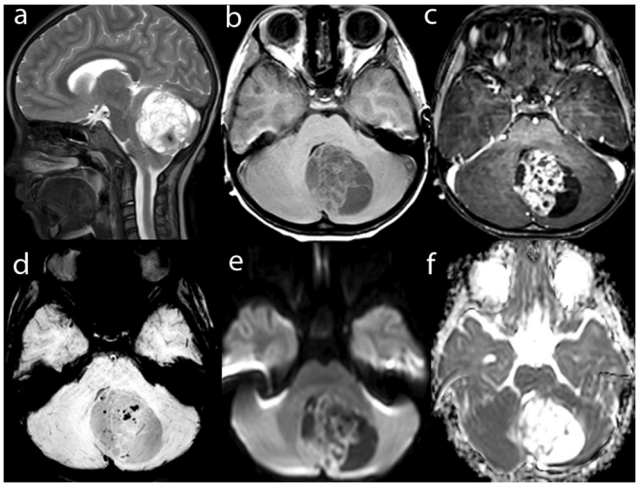

Fig. 1 Preoperative magnetic resonance imaging (MRI). Left paramedian sagittal precontrast T2-weighted image (**a**) shows a cerebellar "bubbly" appearance mass with mixed signal intensity, including hypo- , iso- , and hyperintense signals. .Axial precontrast T1-weighted image (**b**) shows a well-circumscribed mixed solid and cystic mass with predominantly iso- and hypointense signal intensity in the left cerebellovermian area, compressing the 4th ventricle. Axial postcontrast T1-weighted image (**c**) shows a "bubbly" appearance mass caused by enhancing solid portions of the tumor intermixed with internal enhancing cysts. Note the presence of nonenhancing attached cystic component. Axial susceptibility-weighted image (**d**) shows hypointense signal intensity areas with "blooming" artifact which could represent calcifications or hemorrhage. Diffusion-weighted image (**e**) and corresponding apparent diffusion coefficient map (**f**) show no restricted diffusion

restricted diffusion on DWI and corresponding ADC map (Fig. 1). Surgery was done in a prone position with a linear incision extending from the external protuberant to C2 for the median suboccipital craniotomy. Cerebellar tonsils were progressed by using telovelar approach. A solid, soft, and white-pearly left cerebellovermian lesion was found (Fig. 2). The vascularized tumor had a good cleavage from the surrounding brain parenchyma in some areas. Some parts had a limited mass structure that was sticky and irregular. Gross total tumor resection was performed. Histopathological examination revealed a tumor composed of pseudorosettes arranged in papillary fashion. Longitudinal sections of these structures were typically ribbon-like with central sclerotic vessels (Fig. 3a). Pseudorosettes showed broad processes from tumor cell bodies to the adventitia of the central vessels (Fig. 3b). Extensive vascular hyalinization generating numerous pink hyaline rings with scarcely intervening tumor cells was seen with prominent calcification (Fig. 3c). Mitotic activity of the tumor was 2/10HPF. No evidence of increased cellularity, anaplastic nuclear features, microvascular proliferation or necrosis was identified. The Ki67 proliferation index was 3%. GFAP revealed scarce immunopositivity (Fig. 3d) whereas tumor cell cytoplasms were diffusely positive for vimentin (Fig. 1e). INI1 showed diffuse nuclear expression in tumor cells (Fig. 3f). Tumor cells revealed scattered cytoplasmic immunopositivity for S100 and membranous immunopositivity for EMA. Olig2 was diffusely immunopositive in tumor cell nuclei. Neither synaptophysin nor cytokeratin positivity was seen in tumor cells. The tumor was immunonegative for IDH1 and BRAF-V600E. FISH analysis did not reveal 1p/19q co-deletion. Although the diagnosis of AB is very unusual for a tumor in this location, it was made on the basis of the typical histomorphological and immunohistochemical features of the lesion.

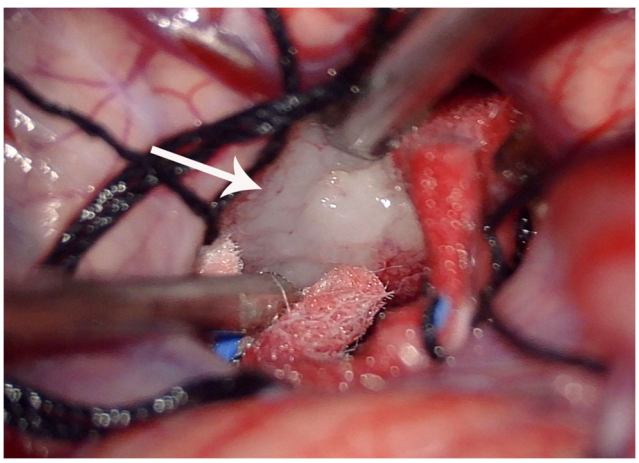

Fig. 2 Intraoperative photograph shows a solid white-pearly tumor

We preferred to perform adjuvant radiotherapy due to the risk of recurrence of this tumor. The patient is disease-free and has been kept on close follow-up for 6 months.

Discussion

The age of AB at diagnosis varies a lot and has been documented in patients ranging from infancy to their 90s [6, 7]. The localization of the majority of the ABs is supratentorial [8–10]. However, the involvement of midbrain, cerebellum, brain stem, and 4th ventricle are rarely reported in the literature [11–16]. In their studies, both Ahmed Ka et al. and Mallick et al. reported that approximately 12% of the patients had a posterior fossa tumor location [7, 18]. Although there was no gender predominance in this review, AB is reported as twice as frequent in female than in male [18]. Clinical signs and symptoms of posterior fossa ABs are nonspecific and depend on the location, size, and mass effect of the neoplasm. They are usually consistent with those associated with elevated intracranial pressure and include headaches, nausea, vomiting, diplopia, dizziness, focal neurological deficits, and balance impairment (Table 1).

Histopathologically, researches have attempted to classify the tumor as a stage in the process of glioma dedifferentiation, as an astrocytoma of large cells producing fibers, or as a rare

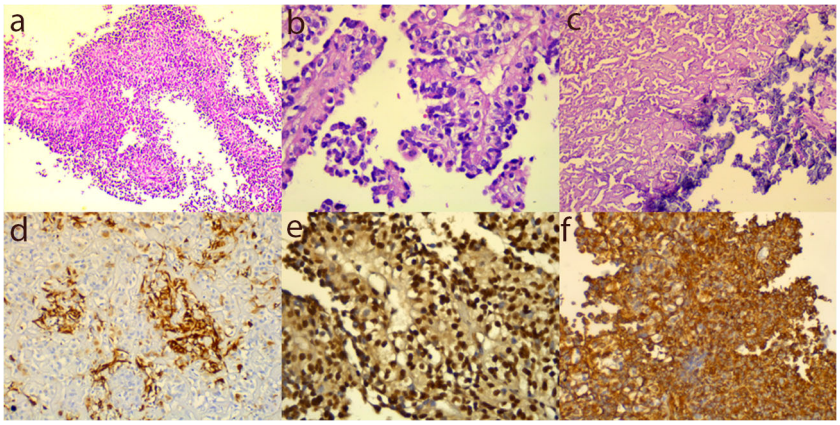

Fig. 3 Histopathological examination. **a** original magnification, × 100, hematoxylin-eosin stain shows cells oriented to central vessels showing variable sclerosis. **b** original magnification, × 400, hematoxylin-eosin stain shows pseudorosettes with broad processes from tumor cell bodies to the adventitia of the central vessels **c** original magnification, × 200, hematoxylin-eosin stain shows prominent vascular hyalinization with calcifications. **d** Original magnification, × 200, GFAP shows scattered cytoplasmic positivity of tumor cells for GFAP. **e** Original magnification, × 200, vimentin shows diffuse cytoplasmic immunopositivity of tumor cells for vimentin. **f** Original magnification, × 400, INI1 shows diffuse nuclear immunoexpression of tumor cells for INI1

tumor, probably originating from tanycytes or ependymal astrocytes [6–8]. Its histogenesis has been explained recently. It is composed of astroblastic elements with circumscription, hyalinization of blood vessels, and a lack of fibrillarity [19, 20]. However, controversies still exist regarding its cellular origin and validity as a distinct entity. ABs can be graded as either a low-grade or a high-grade variant. This histopathologic subclassification was applied by many pathologists but has not yet been integrated into the World Health Organization (WHO) classification [19, 21]. It was first included as a specific entity in the original 1979 WHO classification, but it is listed among "other neuroepithelial tumors" in 2007 WHO Classification of Tumors of the CNS, which does not designate histologic grade [20, 21].

Supratentorial and infratentorial ABs share on imaging characteristics. On MRI, ABs are usually described as hypointense on T1- and hyperintense on T2-weighted images with well-demarcated borders. Calcification is a common imaging feature of the tumor seen in the majority of reported cases [16]. The presence of a "bubbly" appearance caused by the solid parts of the tumor and intermixed multiple cysts may be a characteristic imaging finding, as shown in the current case [8–10]. ABs may show heterogeneous internal enhancement or rim enhancement on postcontrast T1-weighted images. There is usually a mild perifocal edema that usually does not correlate with the grade of the tumor [22, 23]. Although all supratentorial cases discussing DWI had restricted diffusion, our case is the first one showing no restriction on imaging [16].

The main histopathological differential diagnosis of the posterior fossa astroblastoma should include ependymoma, astrocytoma, and angiocentric glioma. Many ependymomas demonstrate true ependymal rosettes, which are generally not seen in ABs. Nuclear immunostaining of tumor cells for Olig2 also appears to exclude most ependymomas. On the other hand, the common histological features of AB, which are usually absent in ependymoma, include frequent multinucleated cells, perivascular cells with nuclear clearing, eosinophilic granular material, lymphocytic infiltrates, rhabdoid cells, hyaline spherical bodies, and nuclear pseudoinclusions. These features are also usually absent in most diffuse gliomas, even though some occur in pilocytic astrocytomas, gangliogliomas, and pilomyxoid astrocytomas. The latter tumors, however, lack extensive astroblastic pseudorosettes and may show other features not found in AB, such as classic Rosenthal fibers, ganglion cells, bipolar spindle cells, or marked pleomorphism [24]. Angiocentric glioma, which is usually found in supratentorial cortical region as nonenhancing ill-defined solid masses, is characterized by perivascular distribution of bipolar and spindle cells, with mild pleomorphism, an infiltrative border, and lack of high-grade features. On immunohistochemical examination, it is typically positive with antibodies to GFAP, S-100 protein, and vimentin. A dot-like pattern of immunoreactivity to EMA has also been described [9]. Tumor cells were immunonegative for synaptophysin; therefore, medulloblastoma was not considered in the differential diagnosis. The classic rhabdoid features and loss of immunoexpression of INI1 which are required for the diagnosis of atypical teratoid/rhabdoid tumor are not seen in ABs. The tumors included in the differential diagnosis do not commonly show the "bubbly appearance" characteristic of astroblastoma on imaging.

Table 1 Reviewed patient's characteristics, MRI features, and treatments of posterior fossa astroblastomas

Study	Age/sex	Location	Symptoms	MRI features	Grade	Treatment	Follow-up recovery
Brat et al. [11]	7/M	Midbrain	Circumscribed mass	-Circumscribed mass	Low	Total resection radiotherapy	7 months full
Navarro et al. [17]	3.3/M	4th ventricle	Headache, focal findings	T1- hypointense, T2- hyperintense, solid with calcifications	Low	Subtotal resection, chemotherapy, radiotherapy	75 months full
Chopra et al. [15]	37/M	Left cerebellar	Headache, balance impairment, vomiting, ataxia	Heterogeneously enhancing solid-cystic mass	Low	Total resection	6 months full
Notarianni et al. [13]	20/F	Brainstem	Left lower extremity numbness, diplopia, blurred vision, ataxia	Well-circumscribed, contrast-enhancing cystic lesion	Low	Total resection	3 months full
Ganapathy et al. [16]	12/F	Vermis, 4th ventricle, brainstem	Headache, vomitimg, dizziness, left 5th and 12th nerve paresis, left upper extremity paresis, ataxia and nystagmus	Heavily calcified solid mass with intense enhancement, Intracranial parenchymal and spinal leptomeningeal metastases	High	Subtotal resection, chemotherapy	–
Shin SA et al. [14]	11/M	Brainstem	Headache, dizziness, photophobia, gait disturbance	Heterogenous and rim enhancing solid and cystic mass,	Intermediate (high Ki 67, focal necrosis +)	Subtotal resection, chemotherapy, radiotherapy	–

Besides histopathologic characteristics, patients should further be classified into low- or high-risk groups depending on features such as age, gender, location, Karnofsky Performance Scale, tumor dimensions, neurologic deficits, BRAF-V600E mutation, Ip and 19q co-deletion, and IDH1 and two mutations to arrange the treatment. It has been found that age over 30, male gender, supratentorial location, and present $BRAF^{V600E}$ mutation were poor prognostic factors [7, 24, 25].

Surgical removal of the tumor with the aim of complete tumor resection is the best treatment of choice. After surgery, observation or adjuvant radiotherapy is generally recommended for the patients at low-risk group, while adjuvant chemoradiotherapy is preferred for high-risk patients [18, 26].

Conclusion

Astroblastoma is an extremely rare condition that may present in the posterior fossa in children. When a characteristic "bubby" appearance enhancing cystic solid tumor is located on the cerebellar hemisphere in a child, an AB may be the most probable diagnosis on imaging.

Compliance with ethical standards

Conflict of interest On behalf of all authors, the corresponding author states that there is no conflict of interest.

References

1. Pizer BL, Moss T, Oakhill A, Webb D, Coakham HB (1995) Congenital astroblastoma: an immunohistochemical study. Case report. J Neurosurg 83:550–555. https://doi.org/10.3171/jns.1995.83.3.0550
2. Bahadur G, Hindmarsh P (2000) Age definitions, childhood and adolescent cancers in relation to reproductive issues. Hum Reprod 15:227–230
3. Sughrue ME, Choi J, Rutkowski MJ, Aranda D, Kane AJ, Barani IJ et al (2011) Clinical features and post-surgical outcome of patients with astroblastoma. J Clin Neurosci 18(6):750–754
4. Bailey P, Cushing HA (1926) A classification of tumors of the glioma group on a histogenetic basis with a correlation study of prognosis. 83–84. Philadelphia, PA: Lippincott 133–136
5. Bailey P, Bucy PC (1930) Astroblastoma of the brain. Acta Psychiatr Neurol 5:439–461
6. Grotts BF (1949) Astroblastoma of the cerebellum in an infant; report of a case. Arch Pediatr 66:283–288
7. Ahmed KA, Allen PK, Mahajan A et al (2014) Astroblastomas: a surveillance, epidemiology, and end results (SEER)-based patterns of care analysis. World Neurosurg 82(1–2):e291–e297
8. Bell JW, Osborn AG, Salzman KL, Blaser SI, Jones BV, Chin SS (2007) Neuroradiologic characteristics of astroblastoma. Neuroradiology 49:203–209
9. Hammas N, Senhaji N, Alaoui Lamrani MY, Bennis S, Chaoui EM, El Fatemi H et al (2018) Astroblastoma - a rare and challenging tumor: a case report and review of the literature. J Med Case Rep 21 12(1):102. https://doi.org/10.1186/s13256-018-1623-1 Review

10. Cunningham DA, Lowe LH, Shao L, Acosta NR (2016) Neuroradiologic characteristics of astroblastoma and systematic review of the literature: 2 new cases and 125 cases reported in 59 publications. Pediatr Radiol 46:1301–1308
11. Brat DJ, Hirose Y, Cohen KJ et al (2000) Astroblastoma: clinicopathologic features and chromosomal abnormalities defined by comparative genomic hybridization. Brain Pathol 10:342–352
12. Kim BS, Kothbauer K, Jallo G (2004) Brainstem astroblastoma. Pediatr Neurosurg 40:145–146
13. Notarianni C, Akin M, Fowler M, Nanda A (2008) Brainstem astroblastoma: a case report and review of the literature. Surg Neurol 69:201–205
14. Shin SA, Ahn B, Kim SK, Kang HJ, Nobusawa S, Komori T, Park SH (2018) Brainstem astroblastoma with MN1 translocation. Neuropathology 20:631–637. https://doi.org/10.1111/neup.12514
15. Chopra I, Roncaroli F, Apostolopoulos V, Moss J, Peston D, O'Neill K. (2007) October 2006: a 37-year old male with headache. Brain Pathol17:251–252
16. Ganapathy S, Kleiner LI, Mirkin DL, Broxson E (2009) Unusual manifestations of astroblastoma: a radiologic-pathologic analysis. Pediatr Radiol 39:168–171
17. Navarro R, Reitman AJ, de León GA, Goldman S, Marymont M, Tomita T (2005) Astroblastoma in childhood: pathological and clinical analysis. Childs Nerv Syst 21(3):211–220
18. Mallick S, Benson R, Venkatesulu B, Melgandi W, Rath GK (2017) Patterns of care and survival outcomes in patients with astroblastoma: an individual patient data analysis of 152 cases. Childs Nerv Syst 33(8):1295–1302
19. Kernohan JW, Mabon RF, Svien HJ et al (1949) A simplified classification of the gliomas. Proc Staff Meet Mayo Clin 24:71–75
20. Zülch KJ (1956) Biologie und Pathologie der Hirn Geschwülste [Biology and pathology of brain tumors]. In: Zülch KJ, Christensen E, editors. Pathologische Anatomie der Raumbeengenden Intrakraniellen Prozesse. Berlin: Springer p. 1–702. German
21. Kubota T, Hirano A, Sato K, Yamamoto S (1985) The fine structure of astroblastoma. Cancer 55:745–750
22. Kim DS, Park SY, Lee SP (2004) Astroblastoma: A case report. J Korean Med Sci 2004(19):772–776
23. de la Garma VH, Arcipreste AA, Vázquez FP, Aguilar RR, Castruita UO, Guerra RM (2004) High-grade astroblastoma in a child: report of one case and review of literature. Surg Neurol Int 2014 24(5):111. https://doi.org/10.4103/2152-7806
24. Lehman NL, Hattab EM, Mobley BC, Usubalieva A, Schniederjan MJ, McLendon RE et al (2017) Morphological and molecular features of astroblastoma, including BRAFV600E mutations, suggest an ontological relationship to other cortical-based gliomas of children and young adults. Neuro-Oncology 19(1):31–42. https://doi.org/10.1093/neuonc/now118
25. Shen F, Chen LC, Yao Y, Zhou LF (2014) Astroblastoma: rare incidence and challenges in the pattern of care. World Neurosurg 82(1–2):e125–e127. https://doi.org/10.1016/j.wneu.2014.03.008
26. Merfeld EC, Dahiya S, Perkins SM (2018) Patterns of care and treatment outcomes of patients with astroblastoma: a National Cancer Database analysis. CNS Oncol 7(2): CNS13. https://doi.org/10.2217/cns-2017-0038